

# Nanocomposite Films Derived from Exfoliated Functional Aluminosilicate through Electrostatic Layer-by-Layer Assembly

Dong Wook Kim,<sup>\*,†</sup> Alexandre Blumstein,<sup>\*,‡</sup> and Sukant K. Tripathy<sup>†,‡,§</sup>

Center for Advanced Materials and Department of Chemistry, University of Massachusetts Lowell, Lowell, Massachusetts 01854

Received January 2, 2001. Revised Manuscript Received March 25, 2001

Multilayered nanocomposite films were prepared from aluminosilicate platelets with functional chromophores and polyelectrolytes through electrostatic layer-by-layer assembly. Fluorescent dye coumarin was intercalated into the layered aluminosilicate hectorite, and the resulting hectorite/coumarin intercalation complex particles were broken down into individual platelets by means of extensive shaking and sonication of their water suspension. Atomic force microscopy (AFM) and transmission electron microscopy data show that the exfoliated platelets have the form of lathes of approximately 10–40 nm width, 150–400 nm length, and 2–3 nm average thickness. This last value is consistent with the overall thickness of a single aluminosilicate lamella sheathed with coumarin molecules on both sides. Given the strong negative surface charge of the aluminosilicate layers, films of nanocomposites could be formed by electrostatic layer-by-layer assembly using a cationic polyelectrolyte. The AFM topography of such films revealed a homogeneous monolayer coverage of the underlying substrate. Linear buildup of the multilayer films of up to 20 cycles was demonstrated and investigated using UV/vis absorption spectroscopy. The resulting transparent films have exhibited strong characteristic blue-green fluorescence due to coumarin dye molecules adhered to the exfoliated hectorite platelets.

## Introduction

Organic/inorganic hybrid core–shell structures based on inorganic nanoparticles are recently stimulating fundamental and applied research for advanced materials with desirable optical, electrical, and magnetic properties.<sup>1–7</sup> The combined unique properties offered by both organic and inorganic components within a single material on a nanoscale level make such nanocomposites attractive for a wide range of applications including next generation optics, optoelectronic nanodevices, chemical or biological sensors, and catalysts. Core–shell nanocomposite particles especially based on structurally well-defined building blocks such as spheres, rigid rods, tubes, and sheets are potentially useful in the preparation of nanoscale devices. While most of the

research has been carried out on the spherical inorganic solids, little attention has been paid to lamellar particles. Considering that uniform ultrathin films with structural order are indispensable for applications, two-dimensional inorganic platelets may be appealing as building blocks for device formation.

Smectite-type aluminosilicates such as montmorillonite or hectorite are characterized by lamellar structure consisting of extremely thin (~1 nm) sheetlike layers. Small cations such as sodium or calcium ions are normally located in the interlayers or galleries to compensate for the negative charge of the silicate layers. Such galleries can offer a two-dimensional nanocavity to accommodate a variety of positively charged species including polymers and organic dye molecules by a simple ion exchange.<sup>8–22</sup> Intercalation of guest mol-

\* To whom correspondence should be addressed.

<sup>†</sup> Center for Advanced Materials.

<sup>‡</sup> Department of Chemistry.

<sup>§</sup> Tragically deceased.

- (1) For a recent review, see: Adair, J. H.; Li, T.; Kido, T.; Havey, K.; Moon, J.; Mecholsky, J.; Morrone, A.; Talham, D. R.; Ludwig, M. H.; Wang, L. *Mater. Sci. Eng. R* **1998**, *R23*, 139.
- (2) Selvan, S. T.; Spatz, J. P.; Klok, H. A.; Moeller, M. *Adv. Mater.* **1998**, *10*, 132.
- (3) Chen, T.-Y.; Somasundaran, P. *J. Am. Ceram. Soc.* **1998**, *81*, 140.
- (4) Selvan, S. T.; Hayakawa, T.; Nogami, M.; Moeller, M. *J. Phys. Chem. B* **1999**, *103*, 7441.
- (5) Caruso, F.; Susha, A. S.; Giersig, M.; Mohwald, H. *Adv. Mater.* **1999**, *11*, 950.
- (6) Harrison, M. T.; Kershaw, S. V.; Rogach, A. L.; Kornowski, A.; Eychmuller, A.; Weller, H. *Adv. Mater.* **2000**, *12*, 123.
- (7) Pastoriza-Santos, I.; Koktysh, D. S.; Mamedov, A. A.; Giersig, M.; Kotov, N. A.; Liz-Marzan, L. M. *Langmuir* **2000**, *16*, 2731.

- (8) Blumstein, A. *Bull. Soc. Chim.* **1961**, 899.
- (9) Blumstein, A. *J. Polym. Sci.* **1965**, *A3*, 2653.
- (10) Vaia, R. A.; Vasudevan, S.; Krawiec, W.; Scanlon, L. G.; Giannelis, E. P. *Adv. Mater.* **1995**, *7*, 154.
- (11) Vaia, R. A.; Giannelis, E. P. *Macromolecules* **1997**, *30*, 8000.
- (12) Hutchison, J. C.; Bissessur, R.; Shriver, D. F. *Chem. Mater.* **1996**, *8*, 1597.
- (13) Oriakhi, C. O.; Lerner, M. M. *Chem. Mater.* **1996**, *8*, 2016.
- (14) Shi, H.; Lan, T.; Pinnavaia, T. J. *Chem. Mater.* **1996**, *8*, 1584.
- (15) Wang, Z.; Pinnavaia, T. J. *Chem. Mater.* **1998**, *10*, 3769.
- (16) Tyan, H.-L.; Liu, Y.-C.; Wei, K.-H. *Chem. Mater.* **1999**, *11*, 1942.
- (17) Weimer, M. W.; Chen, H.; Giannelis, E. P.; Sogah, D. Y. *J. Am. Chem. Soc.* **1999**, *121*, 1615.
- (18) Ren, J.; Silva, A. S.; Krishnamoorti, R. *Macromolecules* **2000**, *33*, 3739.
- (19) Lim, Y. T.; Park, O. O. *Macromol. Rapid Commun.* **2000**, *21*, 231.
- (20) Ishida, H.; Campbell, S.; Blackwell, J. *Chem. Mater.* **2000**, *12*, 1260.

ecules into such host lattices can lead to their ordered molecular arrangement together with a high thermal and oxidative stability. Alternatively, the layered aluminosilicates can be broken down into separate 1-nm-thick sheets through exfoliation. Since the Toyota research group demonstrated that the nylon/layered silicate nanocomposites were an ensemble of uniformly dispersed individual aluminosilicate lamellas produced through exfoliation,<sup>23–26</sup> such hybrid materials have attracted much attention because of their improved thermal and mechanical properties.<sup>27–31</sup>

A practical limitation of the aluminosilicates in applications to devices is their powdery nature. In the conventional route to film by casting an aqueous dispersion of the aluminosilicate and drying it in air, it is difficult to control the thickness of the film and orientation of particles within the film. Pioneering work by Kleinfeld and Ferguson provided a breakthrough to such a problem.<sup>32–35</sup> They first reported the preparation of ordered multilayered films using the exfoliated hectorite platelets and cationic polyelectrolytes through electrostatic self-assembly. Spontaneous layer-by-layer sequential adsorption between oppositely charged species is a well-known method to precisely controlled nanometer-scale composite films.<sup>36–43</sup> Given the strong negative surface charge of the aluminosilicate layers, the layer-by-layer assembly using a positively charged polyelectrolyte is considered as a promising route to the stratified multilayered films. Since then, the two-dimensional aluminosilicate platelets have been recognized as promising nanoscale constructional units for ultrathin nanocomposite films.<sup>44–49</sup>

Exfoliated hectorite with a high aspect ratio of its individual particles makes it easy to conceal some defects of the substrate and hence to obtain the ordered and uniform films.<sup>35</sup> If one can make a single aluminosilicate platelet sheathed with organic chromophores, given the strong negative surface charge of the platelets, the core-shell nanocomposite particles can be assembled into uniform films through layer-by-layer self-assembly using a cationic polyelectrolyte. Then the resulting nanocomposite film may exhibit mechanical strength, solvent resistance, thermal stability, and barrier property given by the silicate platelets as well as desirable optical or electrical properties provided by the proper choice of organic chromophores.

In the previous work, intercalation complexes of the fluorescent dye coumarin and lamellar aluminosilicate hectorite have been prepared and studied.<sup>50</sup> By alternate adsorption of positively charged polyelectrolyte and a negatively charged hectorite/coumarin complex, a multilayered film was also obtained on a glass substrate. The surface topography as observed by atomic force microscopy (AFM), however, revealed that particles of the hectorite/coumarin intercalation complex were aggregated together to reach several micrometers in diameter. As a consequence, the multilayered films became gradually opaque with the number of the deposition cycles. In this work, we prepared a single extremely thin sheet (or thin platelets composed of two to three sheets) sheathed with the organic chromophores by exfoliating the hectorite/coumarin intercalation complex particles. Extensive shaking and sonication of the water dispersion of the layered aluminosilicate hectorite intercalated with the coumarin dye molecules resulted in separate 2–3-nm-thick silicate layers with dye molecules adsorbed on their surface. The shape and size of the platelets were investigated by transmission electron microscopy (TEM) and AFM. Clear transparent multilayered composite films were also obtained by sequential deposition of cationic polyelectrolytes and the two-dimensional platelets of the nanocomposite.

## Experimental Section

**Materials.** Hectorite with a cation-exchange capacity (CEC) of 0.44 mequiv/g (Source Clay Minerals Repository, University of Missouri, Columbia, MO) was purified by traditional sedimentation methods to remove impurities.<sup>51</sup> Coumarin 1 [7-(diethylamino)-4-methylcoumarin] of dye laser grade was purchased from Aldrich and was used without additional purification. An aqueous solution of poly(diallyldimethylammonium chloride) (PDAC; Aldrich,  $M_w = 200\,000\text{--}350\,000$ ) was used for the growth of polycation layers. Deionized water from a Milli-Q system was used in all experiments. The resistivity of the water was higher than 18.2 M $\Omega$ /cm, and the total organic contents were less than 10 ppb. All solid substrates were treated with a Chemsolv solution (aqueous

(21) Huang, X.; Lewis, S.; Brittain, W. J.; Vaia, R. A. *Macromolecules* **2000**, *33*, 2000.

(22) Anastasiadis, S. H.; Karatasos, K.; Vlachos, G.; Manias, E.; Giannelis, E. P. *Phys. Rev. Lett.* **2000**, *84*, 915.

(23) Kojima, Y.; Usuki, A.; Kawasumi, M.; Okada, A.; Kurauchi, T.; Kamigaito, O. *J. Polym. Sci., Part A: Polym. Chem.* **1993**, *31*, 1755.

(24) Kojima, Y.; Usuki, A.; Kawasumi, M.; Okada, A.; Fukushima, Y.; Kurauchi, T.; Kamigaito, O. *J. Mater. Res.* **1993**, *8*, 1185.

(25) Usuki, A.; Kojima, Y.; Kawasumi, M.; Okada, A.; Fukushima, Y.; Kurauchi, T.; Kamigaito, O. *J. Mater. Res.* **1993**, *8*, 1179.

(26) Kojima, Y.; Usuki, A.; Kawasumi, M.; Okada, A.; Kurauchi, T.; Kamigaito, O. *J. Polym. Sci., Part A: Polym. Chem.* **1993**, *31*, 983.

(27) Wang, M. S.; Pinnavaia, T. J. *Chem. Mater.* **1994**, *6*, 468.

(28) Lan, T.; Pinnavaia, T. J. *Chem. Mater.* **1994**, *6*, 2216.

(29) Lan, T.; Kaviratna, P. D.; Pinnavaia, T. J. *Chem. Mater.* **1995**, *7*, 2144.

(30) Chen, T.-K.; Tien, Y.-I.; Wei, K.-H. *Polymer* **1999**, *41*, 1345.

(31) Fournaris, K. G.; Karakassides, M. A.; Petridis, D.; Yiannakopoulou, K. *Chem. Mater.* **1999**, *11*, 2372.

(32) Kleinfeld, E. R.; Ferguson, G. S. *Science* **1994**, *265*, 370.

(33) Ferguson, G. S.; Kleinfeld, E. R. *Adv. Mater.* **1995**, *7*, 415.

(34) Kleinfeld, E. R.; Ferguson, G. S. *Chem. Mater.* **1995**, *7*, 2327.

(35) Kleinfeld, E. R.; Ferguson, G. S. *Chem. Mater.* **1996**, *8*, 1575.

(36) Decher, G. *Science* **1997**, *277*, 1232.

(37) Wang, X. G.; Balasubramanian, S.; Li, L.; Jiang, X. L.; Sandman, D. J.; Rubner, M. F.; Kumar, J.; Tripathy, S. K. *Macromol. Rapid Commun.* **1997**, *18*, 451.

(38) He, J.-A.; Samuelson, L.; Li, L.; Kumar, J.; Tripathy, S. K. *Langmuir* **1998**, *14*, 1674.

(39) He, J.-A.; Valluzzi, R.; Yang, K.; Dolukhanyan, T.; Sung, C.; Kumar, J.; Tripathy, S. K.; Samuelson, L.; Balogh, L.; Tomalia, D. A. *Chem. Mater.* **1999**, *11*, 3268.

(40) He, J. A.; Yang, K.; Kumar, J.; Tripathy, S. K.; Samuelson, L. A.; Oshikiri, T.; Katagi, H.; Kasai, H.; Okada, S.; Oikawa, H.; Nakanishi, H. *J. Phys. Chem. B* **1999**, *103*, 11050.

(41) Ferreira, M.; Cheung, J. H.; Rubner, M. F. *Thin Solid Films* **1994**, *244*, 806.

(42) Lvov, Y.; Ariga, K.; Ichinose, I.; Kunitake, T. *J. Am. Chem. Soc.* **1995**, *117*, 6117.

(43) Lvov, Y.; Haas, J.; Decher, G.; Möhwald, H.; Mikhailov, A.; Mchedlishvili, B.; Morgunova, E. *Langmuir* **1994**, *10*, 4232.

(44) Fendler, J. H. *Chem. Mater.* **1996**, *8*, 1616.

(45) Lvov, Y.; Ariga, K.; Ichinose, I.; Kunitake, T. *Langmuir* **1996**, *12*, 3038.

(46) Laschewsky, A.; Wischerhoff, E.; Kauranen, M.; Persoons, A. *Macromolecules* **1997**, *30*, 8304.

(47) Kotov, N. A.; Haraszti, T.; Turi, L.; Zavala, G.; Geer, R. E.; Dekany, I.; Fendler, J. H. *J. Am. Chem. Soc.* **1997**, *119*, 6821.

(48) Kotov, N. A.; Magonov, S.; Tropsha, E. *Chem. Mater.* **1998**, *10*, 886.

(49) Van Duffel, B.; Schoonheydt, R. A.; Grim, C. P. M.; De Schryver, F. C. *Langmuir* **1999**, *15*, 7520.

(50) Kim, D. W.; Blumstein, A.; Kumar, J.; Tripathy, S. K. *Chem. Mater.* **2001**, *13*, 243.

(51) Akelah, A.; Moet, A. *J. Mater. Sci.* **1996**, *31*, 3589.

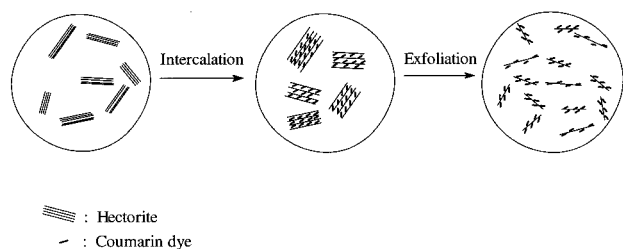


**Figure 1.** Schematic representation for the preparation of the hectorite/coumarin intercalation complex and the exfoliated platelets with coumarin dye.

alkaline alcohol) under sonication.<sup>52,53</sup> Then the substrate was rinsed several times with deionized water. The treatment procedure was used to hydrophilize the substrate and render a net negative charge for subsequent polycation (PDAC) adsorption.

**Intercalation of Organic Dyes into Layered Aluminosilicate.** Coumarin 1 (3 mmol, 0.6930 g) was dissolved in a methanol/water mixture (20 mL/10 mL), and then hydrochloric acid (0.2 N, 15 mL) was added to the solution. The resulting mixture was stirred at 60 °C for 2 h to protonate the dye. A suspension of hectorite (2.278 g) in water was then added to the dye solution, followed by stirring for 24 h. After the dispersion was cooled, the hectorite particles were separated from the solution by a centrifuge and washed several times with deionized water. The resulting slurry was freeze-dried to yield the yellowish hectorite/coumarin intercalation complex. The dye content intercalated into hectorite was estimated by thermogravimetric analysis (TGA).

**Exfoliation of the Hectorite/Coumarin Intercalation Complex Particles.** The intercalation and exfoliation procedures are schematically shown in Figure 1. The hectorite/coumarin intercalation complex particles were dispersed in deionized water at a concentration of 0.1 wt %. The dispersion was shaken for 6–24 h, sonicated for 2–4 h, and then shaken again for an additional 12–24 h. After the unexfoliated particles or aggregates of the exfoliated platelets were separated by a centrifuge, a clear yellowish suspension was obtained. The concentration of exfoliated platelets in their water suspension was determined by measuring the residual solid after evaporating water. The result revealed that 92% of the hectorite/coumarin complex particles was exfoliated and dispersed in the water. The resulting suspension of the exfoliated platelets was clear transparent and quite stable for a period of 1 week.

**Multilayer Films by Layer-by-Layer Deposition.** The overall process of layer-by-layer deposition consists of a cyclic repetition of the following steps: (1) dipping the substrate into an aqueous PDAC solution (typically 0.01 M) for 2 min, (2) rinsing with deionized water and drying with a stream of dry nitrogen, (3) dipping into an aqueous dispersion of the exfoliated hectorite platelets with coumarin dye for 2 min, and (4) final rinsing with deionized water and drying by blowing of dry nitrogen. The buildup of a multilayered film was monitored by UV/vis absorption spectroscopy.

**Characterization and Measurement.** Because water strongly interacts with the negatively charged lamellar platelets of the hectorite, the composites were manipulated and stored in an anhydrous environment. The clay samples were dried at 100 °C for at least 2 h before characterization and measurements. In particular, X-ray data were taken on samples hermetically sealed with a 6- $\mu$ m-thick polypropylene film. The *d* spacing of pure dried hectorite was thus found to be 0.98 nm, close to the theoretical value of 0.96 nm, confirming the effectiveness of the seal.

FT-IR spectra were recorded with a Perkin-Elmer 1600 FT-IR spectrophotometer using KBr pellets. UV/vis spectra were

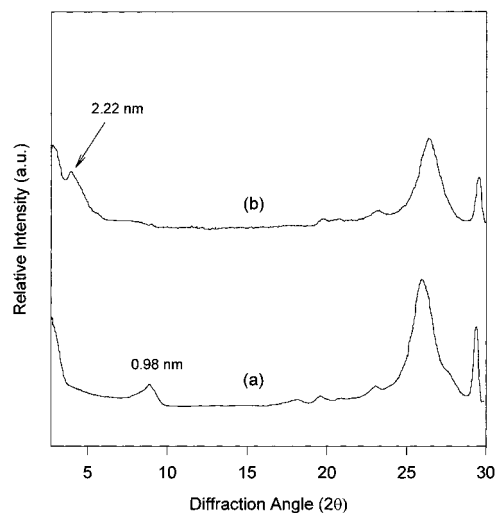


**Figure 2.** Powder XRD patterns of (a) hectorite and (b) the hectorite/coumarin intercalation complex.

taken by means of a GBC UV/vis 916 spectrometer. Emission and excitation characteristics of the samples were measured with an SLM-Aminoco model 8100 spectrofluorometer. The dye content of complexes and their thermal stability were determined by TGA. A TG analyzer TA 2950 (Du Pont) with a sweep from 50 to 800 °C at a heating rate of 10 °C/min was used. The basal (0, 0, *l*) *d* spacings were determined from X-ray diffractograms using Cu K $\alpha$  radiation with a Philips 3-kW X-ray generator and vertical diffractometer. Bright-field TEM images were performed on samples prepared on carbon-covered 200-mesh copper grids, using a Philips EM400T (operating at 120 kV) equipped with a Noran instrument energy-dispersive X-ray spectrometer (EDXS). Surface topography of the nanocomposite films was investigated by an AFM (Park Scientific, CA) operated in the contact mode using a standard silicon nitride cantilever (force constant 0.10 N/m; resonance frequency 38 kHz) in ambient air. The scan rate is 0.5–1.0 Hz, and the set point is 25 nN. The samples for AFM were prepared on silicon substrates by an electrostatic layer-by-layer deposition method.

## Results and Discussion

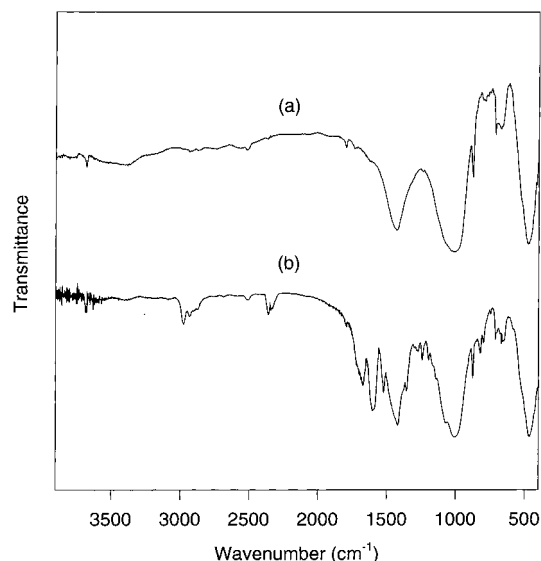
**Intercalation of Coumarin Dye into Hectorite.** Coumarin 1 was treated by an aqueous hydrochloric acid solution because earlier work has shown that such protonated amines can be readily intercalated into the aluminosilicate galleries by an ion exchange.<sup>54</sup> The resulting hectorite/coumarin intercalation complex was investigated using IR, TGA, and X-ray spectroscopy.

Figure 2 compares X-ray diffraction (XRD) patterns of the hectorite/coumarin intercalation complex and pure hectorite. After intercalation, XRD data show that the broad peak centered at 0.98 nm corresponding to the (0, 0, *l*) of pure hectorite was shifted to a new peak at  $\sim$ 2.22 nm. This confirms the insertion of coumarin into the galleries of an expandable lattice of the aluminosilicate. Figure 3 shows the FT-IR spectrum of the hectorite/coumarin intercalation complex along with that of the pristine hectorite. The spectrum of the intercalation complex clearly shows the presence of characteristic absorption peaks due to both organic and inorganic components. The absorption bands at 2900, 1725, and 1610  $\text{cm}^{-1}$  can be associated respectively with

(52) Ariga, K.; Lvov, Y.; Kunitake, T. *J. Am. Chem. Soc.* **1997**, *119*, 2224.

(53) Kim, J.; Wang, H.-C.; Kumar, J.; Tripathy, S. K.; Chittibabu, K. G.; Cazeca, M. J.; Kim, W. *Chem. Mater.* **1999**, *11*, 2250.

(54) Theng, B. K. G. *The Chemistry of Clay–Organic Reactions*; John Wiley & Sons: New York, 1974; pp 211–238.



**Figure 3.** FT-IR spectra of (a) hectorite and (b) the hectorite/coumarin intercalation complex.

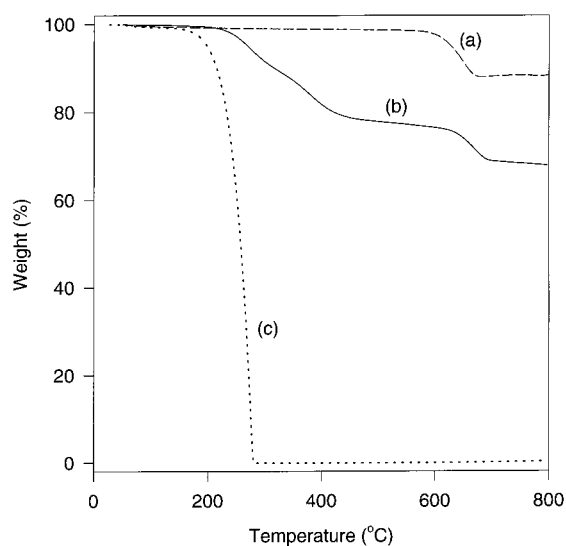


**Figure 4.** TGA of (a) hectorite, (b) the hectorite/coumarin intercalation complex, and (c) coumarin dye. The samples were heated to 800 °C at 10 °C/min in a nitrogen atmosphere.

aliphatic C–H stretching, C=O stretching, and aromatic C=C stretching of the coumarin dye molecules, while those at 1425, 1020, and 480  $\text{cm}^{-1}$  are due to the hectorite.

The content of intercalated coumarin dye could be determined by TGA. Figure 4 shows two distinct regions of weight loss on heating at 230–410 and 600–670 °C. The latter corresponds to the decomposition of a structural  $\text{OH}^-$  group in the aluminosilicate, observed also in the pristine hectorite, while the former must be due to coumarin. The coumarin content was estimated to be 20.4 wt % of the complex, which corresponds to 252% to the CEC of hectorite. We can see that the thermal stability of the intercalated coumarin is significantly enhanced. The onset of weight loss for the intercalated coumarin did not occur until 230 °C, while that for the pure dye began at 150 °C. This enhancement of the thermal stability is attributed to the restricted mobility and spatial confinement within the silicate galleries.<sup>55–58</sup>

**Exfoliation of the Hectorite/Coumarin Intercalation Complex Particles.** It is known that exfoliation

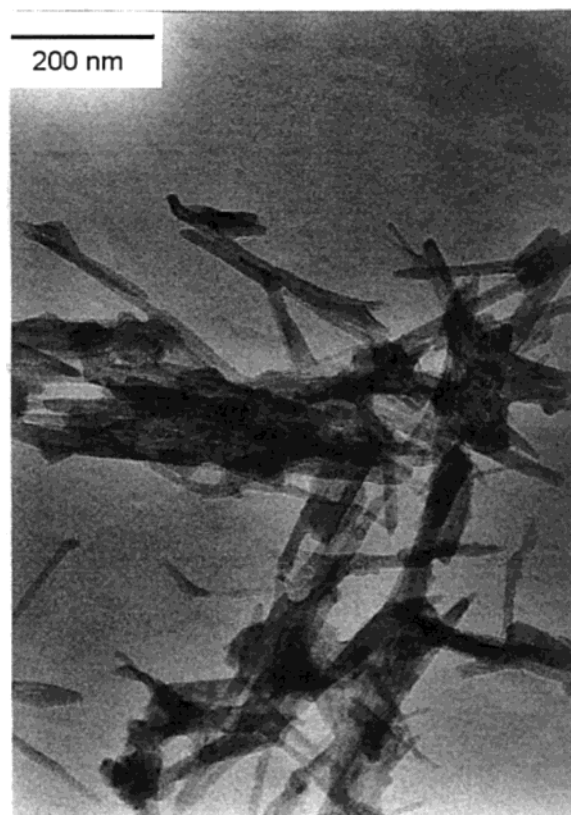


**Figure 5.** TEM image of the exfoliated hectorite platelets with coumarin dye.

of lamellar aluminosilicates is facilitated by expansion through intercalation of organic molecules. To facilitate the exfoliation, we increased the amount of the intercalated coumarin molecules to 252% of the CEC.<sup>59</sup> The exfoliation procedure for the hectorite/coumarin composite was carried out in a way similar to that for the pure hectorite. The exfoliated platelets were obtained by extensive shaking, sonication, and centrifugation as schematically shown in Figure 1. The platelets deposited onto a carbon-covered copper grid were observed using TEM to characterize their shape and size. The TEM image as shown in Figure 5 presents the form of lathes of approximately 10–40 nm width and 150–400 nm length, although some exfoliated platelets aggregated together during the process of sample preparation.

Figure 6 shows AFM images for a monolayer deposition of PDAC and the exfoliated platelets. As can be seen, the exfoliated particles are dispersed randomly and are oriented “flat” on top of the PDAC layer. They are fully covering the surface. There is, however, an occasional overlap of two to four exfoliated platelets. Uniform and structurally ordered ultrathin films are necessary for device applications. With this aim in mind, we made a film using a very diluted suspension of the

(55) Blumstein, A. *J. Polym. Sci.* **1965**, *A3*, 2665.

(56) Mehrotra, V.; Giannelis, E. P.; Ziolo, R. F.; Rogalskyj, P. *Chem. Mater.* **1992**, *4*, 20.

(57) Gilman, J. W.; Morgan, A. *Recent Adv. Flame Retard. Polym. Mater.* **1999**, *10*, 56.

(58) Dultz, S.; Bors, J. *Appl. Clay Sci.* **2000**, *16*, 15.

(59) According to our recent result, exfoliation of the hectorite/coumarin composites with a dye content below 100% of the CEC was found to be much more difficult than those with dye contents over 100% of the CEC (not published). Details about the exfoliation of composites with a different content of dye intercalated into the galleries will be discussed in other reports.

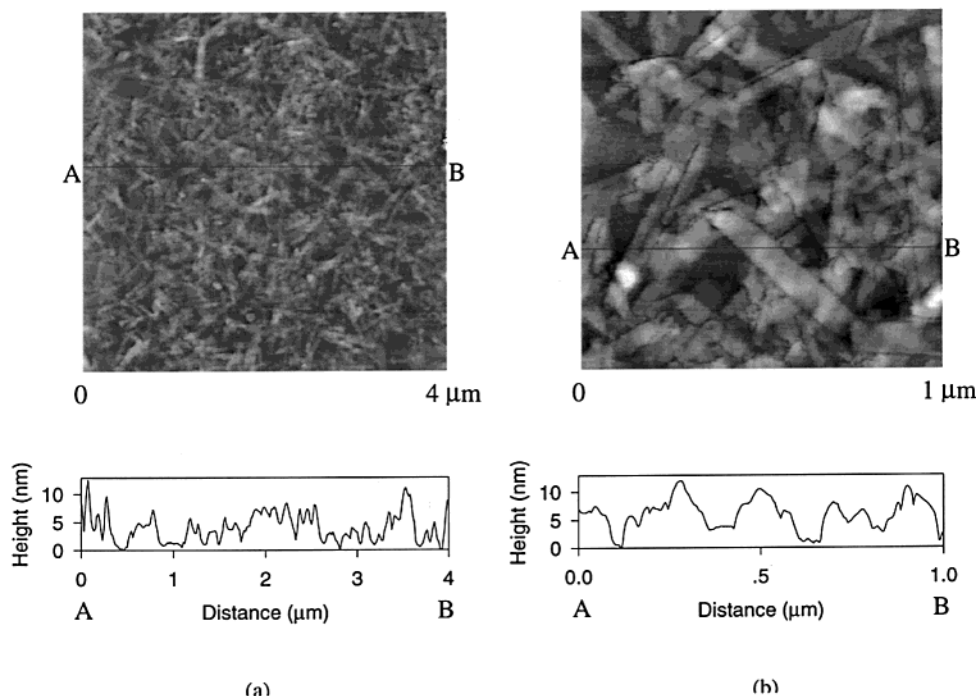


**Figure 6.** AFM images of the one-bilayer composite film after deposition of the exfoliated platelets onto the PDAC layer. Hydrophilized silicon substrate was dipped into a 0.01 M PDAC solution followed by immersion into the water suspension of the platelets (no diluted). The cross-sectional images were taken along the line A–B.

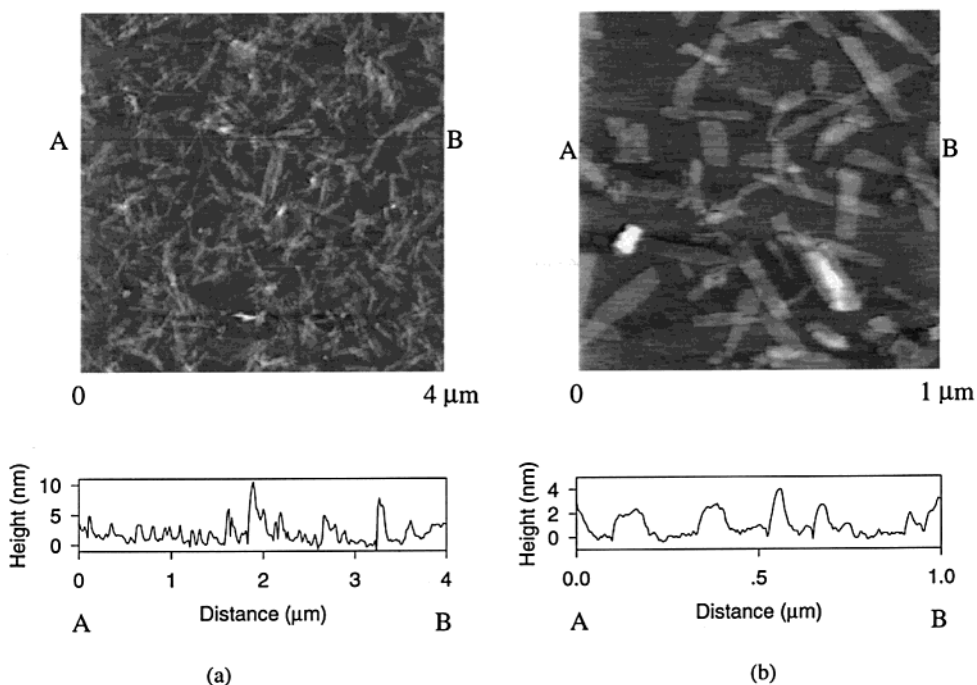


**Figure 7.** AFM images for one-bilayer composite film prepared from a 0.01 M PDAC solution and the water suspension of the exfoliated platelets (10 times the diluted suspension) on the silicon substrates. The cross-sectional images were taken along the line A–B.

exfoliated platelets (10 times the diluted suspension). Figure 7 shows AFM photographs of such films. It indicates that the film is considered to be of almost a monolayer of single platelets. The shapes and sizes of such platelets are consistent with the TEM image. Although it is difficult to give with precision the thickness of the exfoliated lamellar particles because of the limitation of the accuracy of the instrument and the polydispersity of the sample, the average thickness of the single platelets is estimated to be 2–3 nm from the

cross-sectional images. This value is approximately consistent with the overall thickness of the single silicate layer sheathed with coumarin molecules on both sides.

#### Multilayer Films by Layer-by-Layer Deposition.

The adsorption of the platelets on the PDAC layer was found to be quite rapid. After 15 s and after 30 min of exposure to the platelet suspension at the concentration of 0.092 wt %, the resulting films were observed by AFM to have a similar particle surface density.

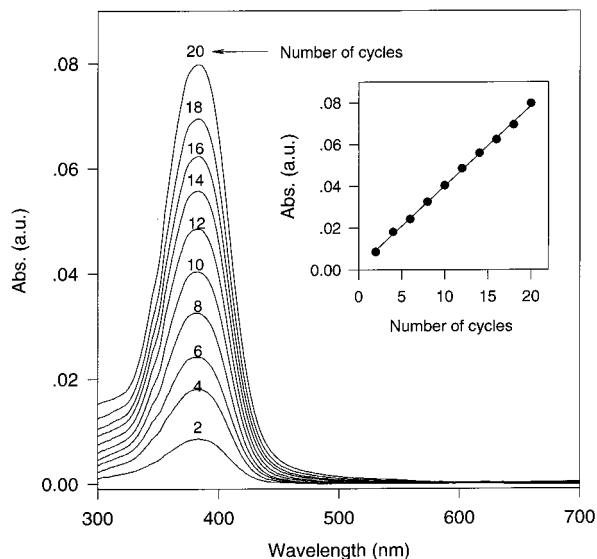


**Figure 8.** Sequential change in the absorbance of the multilayered films with the number of adsorption cycles from PDAC and the exfoliated platelets. The inset shows the linear increase of absorbance with the number of sequential cycles.

The exfoliated platelets may be sheathed with protonated coumarin molecules, which may offset the negative charge of the platelets. In such a case, the nature of the driving force leading to the PDAC/platelets multilayer deposition becomes unclear. Several experiments were performed to reveal the mechanism behind the multilayer deposition. In one case, we tried to deposit the exfoliated platelets on the glass substrate with a negative charge generated by a Chemsolv solution treatment. An AFM study indicated that no platelets were deposited on the glass. In another experiment, multilayer deposition was attempted with anionic polyelectrolyte poly(sodium 4-styrenesulfonate) instead of cationic polyelectrolyte PDAC. As expected, no multilayer deposition was observed from UV/vis absorption spectroscopy and AFM study. Such results indicate that the primary driving force for multilayer deposition is electrostatic.

Multilayered films were prepared by alternate layer-by-layer adsorption of positively charged PDAC and negatively charged platelets on the glass substrates. The resulting composite films are clearly transparent and exhibit a strong green-blue fluorescence on irradiation with 365-nm UV light. Figure 8 shows the absorbance of the film as a function of the number of buildup cycles from PDAC (0.01 M aqueous solution) and the exfoliated aluminosilicate composite sheathed with organic dye (10 times the diluted suspension). Assuming that the absorbance intensity is proportional to the concentration of dye molecules, the buildup of a multilayered film can be estimated from UV/vis absorption spectroscopy. As can be seen from the change of the absorption intensity, the multilayer adsorption of the PDAC/composite assemblies is linear and reproducible with sequential deposition. The absorbance at  $\lambda_{\max}$  ( $\sim 385$  nm) was observed to increase linearly with the number of cycles up to 20 cycles, as shown in the inset of Figure 8.

In the previous work, we have prepared multilayered films from particles of the hectorite/coumarin intercalation complex and PDAC.<sup>50</sup> Such multilayer deposition was also successful as shown in Figure 9. The sequential

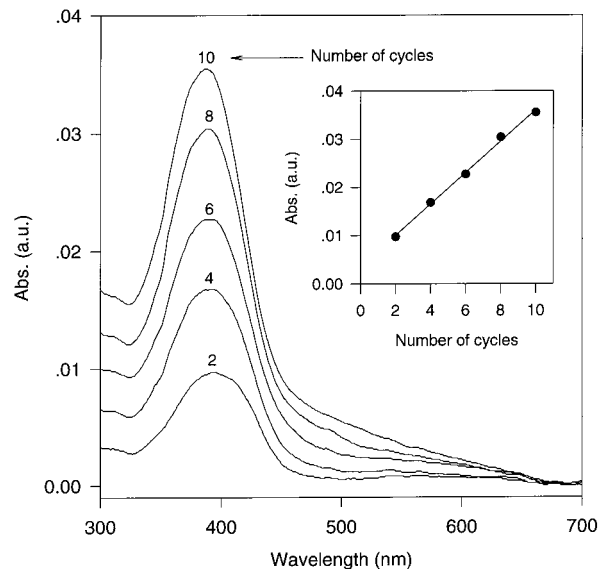


**Figure 9.** Sequential change in the absorbance of the multilayered films with the number of adsorption cycles from PDAC and particles of the hectorite/coumarin intercalation complex.

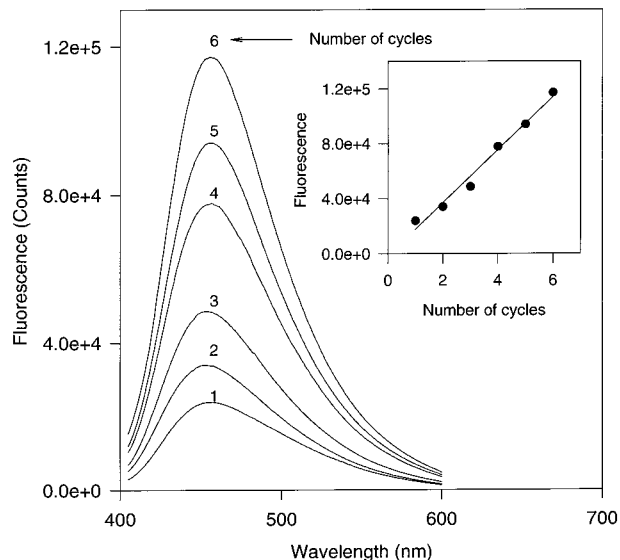


**Figure 10.** Consecutive emission spectra of the multilayered films with the number of adsorption cycles from PDAC and the exfoliated platelets excited at 386 nm. The inset shows the linear relationship between the fluorescence intensity at 465 nm and the number of deposition cycles.

change of absorbance as a function of the number of deposition cycles indicates regular buildup of multilayer films up to 10 cycles. The shape and maximum wavelength of the absorption spectrum in Figure 9 are similar to those of the spectrum in Figure 8. As the layers are built up, however, the short-wavelength side of the baseline becomes gradually tilted as shown in Figure 9. Such a phenomenon may be due to scattering of the incident light by large particles in the films. The surface topography as observed by AFM reveals that particles of the hectorite/coumarin intercalation complex are aggregated together to reach several micrometers in diameter, while the exfoliated composite platelets are too small to scatter the incident light as shown in Figures 6 and 7. This is confirmed by the absence of baseline drift in Figure 8.

The fluorescence spectra of the multilayered nanocomposite film with different numbers of deposition cycles excited at 386 nm were also measured (Figure 10). The nanocomposite film shows a blue emission centered at 465 nm, and the intensity of fluorescence increases almost linearly with the number of sequential deposition cycles. Because hectorite has no chromophores in its structure, such a linear increase of absorption and of the fluorescence intensity indicates that coumarin dye molecules adhere firmly to the exfoliated hectorite platelet and supports AFM data suggesting that the individual exfoliated hectorite platelet is sheathed by coumarin molecules.

### Conclusions

We have described a new strategy for building a nanocomposite film using the exfoliated aluminosilicate with functional organic dye through electrostatic layer-

by-layer assembly. The two-dimensional inorganic sheets with 1-nm thickness can provide a large surface area to accommodate a great amount of functional chromophores. Such organic/inorganic hybrid core-shell nanoparticles may be promising nanostructural building blocks, leading to the ordered ultrathin nanocomposite films having mechanical strength, chemical resistance, thermal stability, and a barrier property through layered architecture and the ionic interaction with the cationic polyelectrolytes. Furthermore, by the proper choice of other functional chromophores, the nanocomposite films may also possess another functionality.

**Acknowledgment.** We thank M. Downey for XRD characterization and Dr. C. Sung for TEM measurement. This work was supported by a Petroleum Research Fund (ACS-PRF 33819-AC5,7).

CM0100016